J.Natn.Sci.Foundation Sri Lanka 2024 52 (1): 69 - 80
DOI: http://dx.doi.org/10.4038/jnsfsr.v52i1.11652

RESEARCH ARTICLE

Modeling and Simulation

Optimal fissile distribution in multiplying systems: Illustrative examples with Monte Carlo simulation and Pontryagin's maximum principle

H Khan[1*], U Aziz[2], ZU Koreshi[2] and SR Sheikh[2]
[1] *National University of Computer and Emerging Sciences (NUCES-FAST), Islamabad, Pakistan.*
[2] *Air University, E-9, Islamabad, Pakistan.*

Submitted: 03 April 2023; Revised: 29 August 2023; Accepted: 22 September 2023

Abstract: In multiplying systems, such as nuclear reactors and criticality experiments, it is desirable to place the fissile material in the optimal or 'best' way to reduce the critical mass of the system as well as to achieve uniform fuel burnup. This paper considers two methods, namely Pontryagin's maximum principle (PMP) and Monte Carlo (MC) perturbation for estimating a minimum critical mass configuration. These methods are applied to an elementary multizone model of a pressurized water reactor (PWR) and a criticality experiment to estimate the minimum critical mass. It is found that while two-group diffusion theory with PMP predicts a minimum critical mass, more detailed MC simulations with MCNP5 show a consistent reduction in critical mass when fissile fuel is placed in inner zones. Such a distribution reduces the fissile material requirement but is undesirable due to the higher power peaking. MC simulations show that for a three-zone model of the KORI 1 PWR, a uniform fissile distribution gives criticality for 1.09 atomic percent (at.%) enrichment, whereas non-uniform fissile distribution (0.6, 1.6, 0.6 at.%) reduces the critical mass by 14%. The changes found from MC simulations were subsequently predicted from first- and second-order derivative sampling. It was found that substantial computational savings can be achieved for large-scale optimization problems. In the case of a criticality experiment, MC derivative sampling was also used to estimate optimal fissile distribution for minimizing the critical mass.

Keywords: Derivative sampling, Goertzel's distribution, MCNP, minimum critical mass, Pontryagin maximum principle.

INTRODUCTION

The concept of minimum critical mass (MCM) (Goertzel, 1956) has been a challenging and interesting research topic over the last few decades, beginning with Goertzel's two-group diffusion theory model, and including work by Wilkins (Wilkins Jr. & Srivastava, 1982), Williams (Williams, 2003; 2017) and others based on the transport model.

Critical mass refers to the minimum amount of fissile material required for a self-sustaining nuclear chain reaction. It is a fundamental concept in nuclear physics that ensures a stable and controlled reaction. The concept was systematically explored for the first time during the Manhattan Project (Gosling, 1999). Enrico Fermi and his team explored the relation between the amount of fissile material and the rate of fission reactions (Segrè, 1970). The construction of the first controlled experimental nuclear reactor Chicago Pile-1, in 1942, demonstrated the significance of both the placement and quantity of fissile material for achieving a self-sustainable nuclear chain reaction (Rowinski *et al.*, 2015).

This concept gained further validation through subsequent nuclear tests, most notably the Trinity test in 1945 (Szasz, 1984). The understanding of critical mass is not only crucial for the development but also for the

* Corresponding author (hamda.khan@nu.edu.pk; https://orcid.org/0009-0002-2266-3908)

safe operation of nuclear reactors. Advancements in nuclear physics have refined the concept, incorporating considerations such as reflectors and control rods. This enhanced understanding has led to the concept of MCM, which reduces the required amount of fissile material even further for a self-sustaining nuclear chain reaction.

Goertzel concluded that a necessary condition for MCM in a reflected reactor is a flat thermal flux while literature shows that the necessary condition is that the integral of the product of the thermal neutron flux and a function related to the adjoint flux is a constant. The thermal flux flattening has also been shown for diffusion theory (Lewins, 2004) for heterogeneous systems of thin fuel 'foils' in a moderator (Dam, 2013; 2015). The basic purpose of non-uniformly distributing the fuel is to achieve criticality with a minimum amount of fissile material. For a nuclear power reactor, the placement of fuel rods in an optimal pattern is both an engineering and economic objective for achieving efficient fuel utilization and scheduled fuel reloading. A power reactor such as the AP1000, for example, has 157 fuel assemblies with a 17 × 17 rod array containing 41,448 fuel rods of three enrichments. To place these optimally is a large-scale optimization challenge that requires efficient methods and computational techniques. Thus, theoretical works which are mostly based on models with assumptions and artifacts are of great value; hence the motivation for this work. An idealized model of a PWR is considered for an optimization study using Monte Carlo (MC) simulation with the MCNP5 (Briesmeister, 2003) code. Apart from its use as a production code with detailed physics modeling, 'continuous' cross-section data libraries, and combinatorial 3D geometry modeling, the perturbation capability is particularly useful for sensitivity analyses and design optimization.

This work uses derivative sampling for illustrative cases to predict optimality from a 'reference' design; computational efficiency depends on how 'good' a reference is. To this end, a two-group diffusion model with the Pontryagin maximum principle (PMP) (Lee, 1973; Koreshi *et al.*, 2019) variational formulation can be used.

This paper considers two applications, namely a multi-zone bare cylindrical reactor, and a criticality experiment to obtain 'optimal' configurations with MC derivative sampling leading to minimization of critical mass. These outcomes are discussed in connection with Goertzel's result that more fissile material should be added to the central regions and progressively less material towards the end of the core region.

For a three-zone bare reactor, a two-group PMP formulation shows (Lee, 1973) an optimal configuration associated with minimum critical mass in a min-max-min (enrichment) fissile distribution. Such a configuration can also be predicted using sensitivity coefficients from MC derivative sampling based on the importance (Otsuka, 2017) of a zone to decide whether fissile material should be added or removed. This strategy is used in this paper to estimate the optimal fissile distribution for a criticality experiment by Clark (Clark, 1966) and also to demonstrate MCM in a U^{235}-H_2O system.

METHODOLOGY

The formulations considered for estimating MCM are two-group diffusion theory with PMP, and MC simulation with derivative sampling.

Notations used in the paper are defined in the Annex 1

Two-group diffusion model

In the two-group diffusion equations for a bare multiplying system (Lamarsh & Baratta, 2001)

$$D_1\nabla^2\phi_1 - \Sigma_1\phi_1 + \frac{k_\infty}{p}\Sigma_2\phi_2 = 0 \qquad ...(01)$$

and

$$D_2\nabla^2\phi_2 - \Sigma_2\phi_2 + p\Sigma_1\phi_1 = 0, \qquad ...(02)$$

for a uniformly distributed fuel, the coefficients in equations. 1 and 2 are constant. These equations can be solved to obtain exact solutions by applying the usual boundary conditions at the center, interfaces, and outer boundary for a multizone cylindrical reactor.

The optimal fissile nuclide distribution can be estimated from a variational formulation (Lee, 1973; Koreshi *et al.*, 2019; Saracco *et al.*, 2019), based on the above two-group diffusion equations. For a bare multizone reactor equations (1) and (2) are written with $D_1, D_2, \Sigma_1, \Sigma_2$ constant in each zone. The thermal absorption cross-section is expressed as a 'control' parameter u where $\Sigma_{2c} \equiv u = \gamma u' + \delta$, where u' is the atomic enrichment $u' = \frac{N^{235}}{N^U}$. The total number of uranium atoms $N^U = N^{235} + N^{238}$, is kept constant, while the enrichment is varied. Here $\gamma = N^U\sigma_{2F}^5$, and $\delta = \Sigma_{2,others}$ where 'others' represent the moderator, structural material, zirconium, etc.

The optimization problem is then formulated as:

$$\text{minimize } \tilde{J} = \int u(r)\, dV \qquad ...(03)$$

$$\text{subject to } N^U = constant$$

In the variational formulation (Lee, 1973), equations (1) and (2) are written as four first-order state-space equations for variables y_i, where $i = 1,2,3,4$, and with a performance index $\tilde{J}$, given as equation (3), defined as a function with 'control' u representing fissile mass in volume V, to be minimized.

The 'augmented' Hamiltonian can then be written as

$$H = \sum_{i=0}^{5} \varphi_i f_i \left(\underline{y}, u, x\right) \qquad ...(04)$$

where φ_i are adjoint functions and φ_0, f_0 represent $\tilde{J}$. From the stationarity conditions on H, coupled ODEs are obtained for λ_i and f_i and solved with the transversality conditions. Pontryagin's Maximum Principle, with admissible controls $u = u_m, u_M$ (minimum and maximum values) is subsequently expressed in the form

$$H = \psi_1(u,x) + \psi_2(x). \qquad ...(05)$$

Thus, in a bare multizone reactor, u is selected such that H is maximized and the shape of the 'switching function' $\psi_1(u,x)$, obtained from λ_i and f_i, determines the controls. Such an analysis leads to critical configurations in a multizone analysis. The MCM, for this 'restrictive criticality configuration', is subsequently found for (u_M, u_m) fuel enrichments in the inner and outer zones of a two-zone core while a (u_m, u_M, u_m) configuration is found in a three-zone core.

In a single zone, there is no optimal arrangement, and the criticality condition is given as

$$\left| J_0(\mu R)\; I_0(\lambda R)\; S_1 J_0(\mu R)\; S_2 I_0(\lambda R) \right| = 0 \qquad ...(06)$$

where J_0 is zero-order Bessel function and I_0 is modified zero-order Bessel functions, μ^2 and λ^2 are constants given as equations (7) and (8) and $\tau_1 = \frac{D_1}{\Sigma_1}$, $\tau_2 = \frac{p\Sigma_1}{D_2}$, $\alpha = \frac{k_\infty}{pD_1}$, $\beta = 1/D_2$.

$$\mu^2 = \frac{1}{2}\left[-\left(\beta u + \frac{1}{\tau_1}\right) + \sqrt{\left(\beta u + \frac{1}{\tau_1}\right)^2 + 4u\left(\frac{\alpha}{\tau_2} - \frac{\beta}{\tau_1}\right)}\right] \qquad ...(07)$$

$$\lambda^2 = \frac{1}{2}\left[+\left(\beta u + \frac{1}{\tau_1}\right) + \sqrt{\left(\beta u + \frac{1}{\tau_1}\right)^2 + 4u\left(\frac{\alpha}{\tau_2} - \frac{\beta}{\tau_1}\right)}\right] \qquad ...(08)$$

$S_{1,2}$ are the coupling coefficients $S_1 = \tau_2(\mu^2 + \beta u)$, $S_2 = -\tau_2(\lambda^2 - \beta u)$.

For a two-zone bare cylindrical reactor, the MCM arrangement requires (u_M, u_m) configuration. In a three-zone reactor, with regions I, II, and III for $0 \le r \le r_1$, $r_1 \le r \le r_2$ and $r_2 \le r \le R$, a criticality configuration is obtained by finding values of minimum enrichment u_m and maximum enrichment u_M in the configuration u_m, u_M, u_m from the determinant of the $10X10$ matrix given in equation 9. The three-zone matrix is given as

$$\begin{bmatrix}
S_{11}J_0(\mu_1 r_1) & -S_{21}J_0(\mu_2 r_1) & 0 & -S_{22}Y_0(\mu_2 r_1) & 0 & S_{13}I_0(\lambda_1 r_1) & -S_{23}I_0(\lambda_1 r_1) & 0 & -S_{24}K_0(\lambda_2 r_1) & 0 \\
-S_{11}\mu_1 J_1(\mu_1 r_1) & S_{21}\mu_2 J_0(\mu_2 r_1) & 0 & S_{22}\mu_2 Y_1(\mu_2 r_1) & 0 & S_{13}\lambda_1 I_1(\lambda_1 r_1) & 0 & 0 & -S_{23}\lambda_1 I_1(\lambda_1 r_1) & 0 \\
0 & S_{21}J_0(\mu_2 r_2) & -S_{31}J_0(\mu_1 r_2) & -S_{22}Y_0(\mu_2 r_2) & -S_{32}Y_0(\mu_1 r_2) & 0 & S_{23}I_0(\lambda_2 r_2) & -S_{33}I_0(\lambda_1 r_2) & S_{24}K_0(\lambda_2 r_2) & -S_{34}K_0(\lambda_1 r_2) \\
0 & -S_{21}\mu_2 J_1(\mu_2 r_2) & S_{31}\mu_1 J_1(\mu_1 r_2) & -S_{22}\mu_2 Y_1(\mu_2 r_2) & S_{32}\mu_1 Y_1(\mu_1 r_2) & 0 & S_{23}\lambda_2 I_1(\lambda_2 r_2) & -S_{33}\lambda_1 I_1(\lambda_1 r_2) & -S_{24}\lambda_2 K_1(\lambda_2 r_2) & S_{34}\lambda_1 K_1(\lambda_1 r_2) \\
J_0(\mu_1 r_1) & -J_0(\mu_2 r_1) & 0 & -J_0(\mu_2 r_1) & 0 & I_0(\lambda_1 r_1) & -I_0(\lambda_2 r_1) & 0 & -K_0(\lambda_2 r_1) & 0 \\
-\mu_1 J_1(\mu_1 r_1) & \mu_2 J_1(\mu_2 r_1) & 0 & \mu_2 Y_1(\mu_2 r_1) & 0 & \lambda_1 I_1(\lambda_1 r_1) & -\lambda_2 I_1(\lambda_2 r_1) & 0 & S_{24}\lambda_2 K_1(\lambda_2 r_1) & 0 \\
0 & J_0(\mu_2 r_2) & -J_0(\mu_1 r_2) & -Y_0(\mu_2 r_2) & -Y_0(\mu_1 r_2) & 0 & I_0(\lambda_2 r_2) & -I_0(\lambda_1 r_2) & K_0(\lambda_2 r_2) & -K_0(\lambda_1 r_2) \\
0 & -\mu_2 J_1(\mu_1 r_2) & \mu_1 J_1(\mu_1 r_2) & -\mu_2 Y_1(\mu_2 r_2) & \mu_1 Y_1(\mu_1 r_2) & 0 & \lambda_2 I_1(\lambda_2 r_2) & -\lambda_1 I_1(\lambda_1 r_2) & -\lambda_2 K_1(\lambda_2 r_2) & \lambda_1 K_1(\lambda_1 r_2) \\
0 & 0 & S_{31}J_0(\mu_1 R) & 0 & S_{32}Y_0(\mu_1 R) & 0 & 0 & S_{33}I_0(\lambda_1 R) & 0 & S_{34}K_0(\lambda_1 R) \\
0 & 0 & J_0(\mu_1 R) & 0 & Y_0(\mu_1 R) & 0 & 0 & I_0(\lambda_1 R) & 0 & K_0(\lambda_1 R)
\end{bmatrix} \qquad ...(9)$$

where Y_0 is zero-order Bessel function and K_0 is a modified zero-order Bessel function. S_{ij} are the coupling coefficients for zone i and index j with $S_{11} = S_{21} = S_{22} = S_1, S_{13} = S_{23} = S_{24} = S_2$.

The condition for the determinant is Cramer's rule for the solution of a system of linear homogeneous equations. The equations arise out of four continuity conditions for flux and current at the interfaces r_1, r_2 and two zero-flux continuity conditions at the outer boundary R.

The homogeneous system of linear equations is thus solved for pairs of minimum and maximum enrichment values that correspond to criticality; one of these pairs $\underline{u}^* = (u_m, u_M, u_m)^*$. The condition that inner and outer zones have the same enrichment is a restriction imposed here which makes this criticality analysis different from that of Goertzel for which a continuous distribution is obtained. The optimal distribution is thus piece-wise continuous with fissile atomic densities contained in the 'optimal' control $\underline{u}^*$.

MC Simulation with derivative sampling

The optimal distribution $\underline{u}^*$ can be found using MC simulation by sampling derivatives (Rief, 1984; Koreshi & Lewins, 1990) in a 'reference configuration'; computational speed-up can be achieved by estimating the reference from a diffusion-based variational described in the preceding section.

Derivatives in an MC simulation are 'scored' during a 'history' in analog simulation from 'birth' to 'death'; the scores are based on the integral form of the transport equation. The collision density $\chi(P)$ in phase space $P(r, E, \hat{\Omega}, t)$ is given as

$$\chi(P) = S(P) + \int K\left(P' \to P\right)\chi\left(P'\right)dP' \quad ...(10)$$

where $S(P)$ is the 'direct source' in P, and $K(P' \to P)$ is the transition kernel describing a neutron transition from $P' \to P$. This kernel $K(P' \to P)$ is expressed as the product of a 'collision' part, and a 'transport' part

$$K = \hat{C} \cdot \hat{T} \quad ...(11)$$

so that the change in quantity such as k_{eff} can be estimated due to a perturbation in a parameter p by a Taylor series expressed as

$$k_{eff}(p) = k_{eff}(p_o) + \frac{dk_{eff}}{dp}|_{p_o}\delta p + \frac{1}{2!}\frac{d^2k_{eff}}{dp^2}|_{p_o}(\delta p)^2 + \cdots \quad ...(12)$$

Optimization using MC derivatives

The MC derivatives sampled for a zone can be interpreted as 'sensitivity' coefficients for that zone. Thus, the material is preferably placed in a zone of high importance and removed from a zone of low importance. This can lead to a net reduction in total fissile material in a critical system. The optimal distribution $\underline{u}^*$ can then be found by an optimization search to yield the MCM.

The optimization problem is thus expressed as

$$\text{minimize } \tilde{J} = m_{ref} + \sum_{i=1}^{N} \Delta m_i \quad ...(13)$$

$$\text{subject to } \sum_{i=1}^{N} \Delta m_i \frac{\partial k_{eff}}{\partial \Delta m_i} = 0 \quad ...(14)$$

where $m_{ref}, and\ \Delta m_i$ are the fuel mass in the reference design, and the mass added or removed from zone *i* respectively.

RESULTS AND DISCUSSION

Bare cylindrical reactor

For the decommissioned Korean (Westinghouse) KORI-1 Reactor (Clark, 1966), a bare cylindrical U-H_2O homogeneous model is considered of radius 122.6 cm, height of 365.8 cm with a fixed number of U atoms $N^U = N^{235} + N^{238}$ = 6.994 × 10^{21} atoms cm^{-3}, the number of oxygen atoms in uranium N^U_{Oxygen} = 1.399 × 10^{22} atoms cm^{-3}, $and\ N_w$ = 1.947 × 10^{22} molecules cm^{-3}. The two-group data are $D_1 = 1.367\ cm$, $D_2 = 0.2294\ cm$, $\Sigma_{1s} = 0.03922\ cm^{-1}$, and $\Sigma_{2c}^{others} = 0.028058\ cm^{-1}$.

The mass of U^{235} (in grams for volume V in cm^3) in terms of the enrichment *u* is

$$M_5 = 235.04\frac{uN_UV}{N_{av}} \sim uV \quad ...(15)$$

which is proportional to *u* for equal volume zones.

The one-zone two-group criticality determinant (equation 6) gives criticality at 1.10% enrichment compared with MCNP5 simulations, for 1000 neutrons simulated for 1000 cycles with 10 skip cycles, shown in Figure 1 giving k_{eff} = 1.00029 (0.00052) at 1.09% (513.96 kg U^{235}) and 1.00422 (0.00053) at 1.1% (518.68 kg U^{235}) and associated values of fissile mass. The cross-sections were taken from the ENDF66a and ENDF66c libraries of MCNP5.

Table 1 lists the criticality pairs and associated relative critical masses m_r defined as $(u_M + 2u_m)/(u_M + 2u_m)_o$ where the subscript *o* denotes the critical pair at 1.09 at.%, obtained from MC simulations, for a three-zone bare critical reactor (radii 70.7831 cm, 100.1025 cm, 122.6 cm, height 365.8 cm).

Table 1: Criticality pairs and critical mass

u_M (%)	1.09	1.15	1.20	1.30	1.40	1.50	1.60
u_m (%)	1.090	1.0665	1.050	0.981	0.877	0.75	0.600
k_{eff}	1.00029 (0.00052)	1.00006 (0.00053)	1.00092 (0.00055)	1.00002 (0.00053)	1.00090 (0.00055)	1.00050 (0.00055)	1.00039 (0.00058)
m_r	1.00	1.00	1.01	1.00	0.96	0.92	0.86

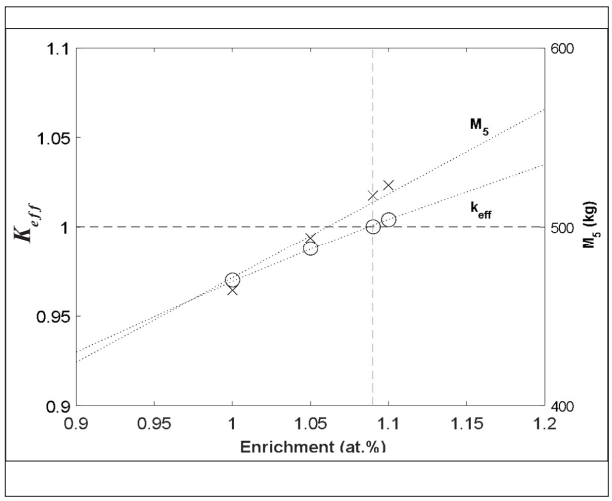

Figure 1: Effective multiplication k_{eff} and fissile mass in the KORI-1 cylindrical reactor

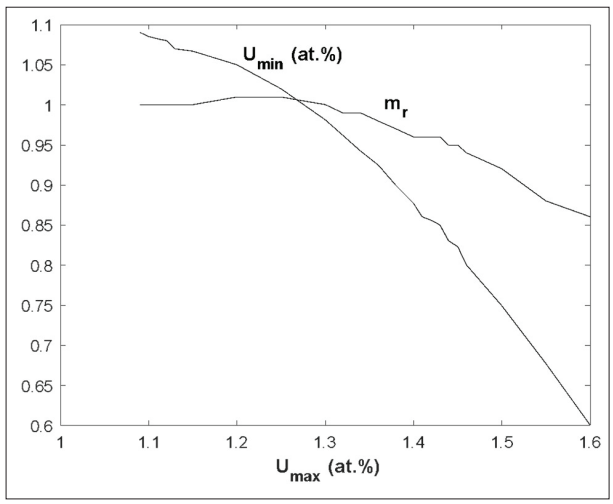

Figure 2: Critical pairs and relative critical mass

The results show that the relative critical mass remains steady till u_M is increased from 1.09 to 1.25 ($u_m = 1.02$) then falls to 0.86 for the min-max pair (0.60, 1.60) as shown in Figure 2. As u_M is increased to 1.8%, u_m decreases to 0.33% with m_r falling to 0.75. The critical mass can thus be reduced by 25% in this configuration. Beyond this, MC simulations give a critical configuration of u_M = 1.85% in the central zone surrounded by water in the inner and outer zones.

In the above simulations, the enrichments in the first and third zones were kept equal to compare with the 10 ×10 critical determinant obtained by Lee in the PMP formulation. This was shown by Lee to result in 'switching functions' requiring a u_m, u_M, u_m configuration for minimizing critical mass in a three-zone reactor.

As stated before, LWRs typically have fuels of three levels of enrichment, with the lowest enrichment fuel in the innermost zone followed by the next higher enrichment fuel and the highest enrichment in the outer zone. The Westinghouse KORI reactor, modeled by Lee in the preliminary PMP formulation, also had fuels of three levels of enrichment (2.10, 2.83, and 3.20 weight %) so that the outer zone does not have the same enrichment as the innermost zone. The Westinghouse AP1000 has three fuels of enrichment 2.35, 3.40, and 4.45 weight % with an initial core loading consisting of interspersed lower enrichment fuels and the outer periphery containing the highest enriched fuel. Such a distribution gives a favorable radial power distribution.

The MCNP simulations for the critical pairs reported by Lee using two-group diffusion theory give the following results: for the pairs (0.9, 0.89), (1.1, 0.71), (1.2, 0.65), (1.3, 0.61), (1.40, 0.58), and (1.50, 0.56) the estimates are k_{eff} = 0.92734 (0.00049), 0.92043 (0.00052), 0.93317 (0.00052), 0.94748 (0.00054), 0.96205 (0.00055), and 0.978978 (0.00056), respectively. By including structural materials, these estimates are likely to decrease. Thus,

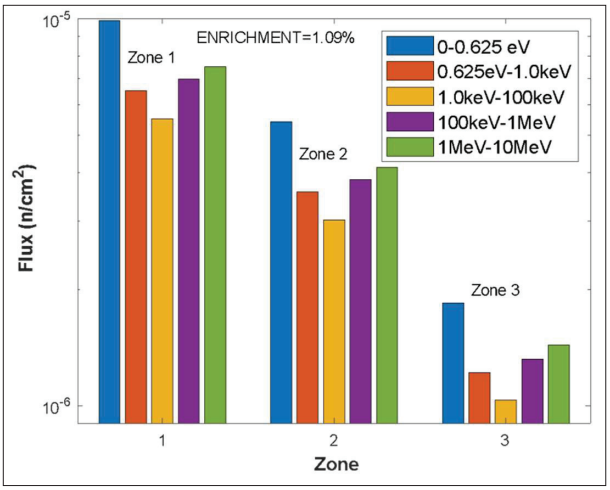

Figure 3: Group fluxes in for uniform fissile (1.09 atomic %) distribution

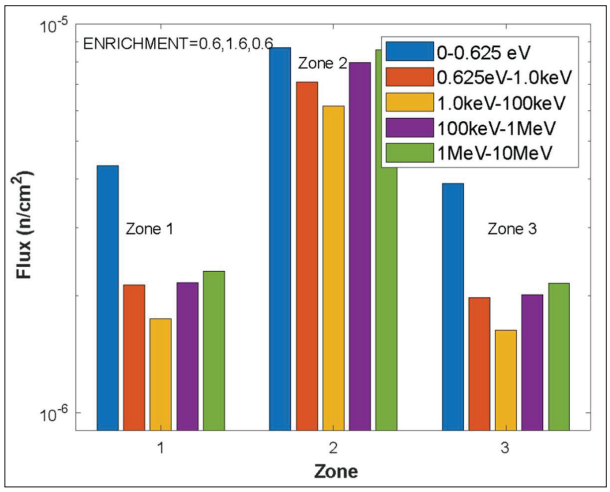

Figure 4: Group fluxes in for 0.6, 1.6, 0.6 atomic % distribution

the present MC simulations differ significantly from the two-group diffusion results of Lee. The relative critical masses for these pairs (1.00, 0.94, 0.93, 0.94, 0.96, and 0.98, respectively) led Lee to report a minimum critical mass.

We next consider the two pairs in Table 1 which give a 14% decrease in critical mass to see what effect they have on the relative fluxes in the zones. These results are shown in Figure 3 and Figure 4.

As seen from Figure 3 and Figure 4, in reducing the critical mass by increasing the fissile fuel in the central zone, the fluxes show a decrease in the inner zone and an increase in the central and last zones; the outer zone is now almost as 'good' as the inner zone. The problem now, clearly, is the increased peaking in the central zone. The ratios of thermal flux in the first zone to the second and third zones in Figure 3, 1.83 and 5.38, respectively, have now changed to 0.50 and 1.11. An intuitive remedy is the reduction of the central zone which will bring the flux down favorably but would need to be compensated by additional fuel in the outer zone. The decision of how much to remove from one zone and add in the other could be made based on the zone 'importances'.

From the MCNP5 neutron activity table for the results of Figure 4, we see that about 60% of the collisions take place in the central zone and 20% each in the inner and outer zones; the activity is thus three times enhanced in the central zone. Both the number-weighted energy and the flux-weighted energy are higher in the central zone as well. The aim should thus be to reduce the central zone activity by a third and compensate for criticality by additions in the inner and outer zones.

By now it is well established that the fuel should be distributed such that the product of the thermal flux and the adjoint thermal flux should be a constant. Of course, that applies to a core-reflector configuration for which the constant in the core should not exceed that constant in the reflector. In our case, we have a bare homogenous reactor instead of a reflected reactor.

We now take the help of MC derivative sampling to estimate the sensitivity of the central zone. The MC derivatives were sampled with the following commands:

PERT1:N CELL=2 MAT=1090 to estimate the derivatives and changes in reducing the central zone enrichment from 1.6% to 1.09%, and

PERT2:N CELL=1,3 MAT=1090 to estimate the derivatives and changes in increasing the first and third zone enrichments from 0.6 to 1.09%. The identifier MAT=1090 denotes material with an enrichment of 1.09%.

The estimates for PERT1 and PERT2, for the predicted change in k_{eff} (track length flux estimator) are $-0.08181\ (0.00005)$ and $0.06901\ (0.00003)$ respectively for the MC simulation with 5000 neutrons sampled in 5000 cycles with 10 skip cycles. These add up to give a predicted change of about -0.01 whereas the

total is zero since both are critical configurations. The estimates are nonetheless useful as they are two 'stand-alone' estimates while the change is simultaneous. The simulation also gives predicted estimates in the track length scalar fluxes in each energy bin shown in Figure 3 and Figure 4. Thus, the full range of critical configurations can be predicted with reasonable accuracy.

Optimization

Derivatives estimated in a 'reference' MC simulation are used to estimate the amount of fissile material to be added or removed from each zone. For perturbations in a three-zone reactor with 172.893 kg U^{235} in each zone, the actual and predicted changes, with relative standard error (RSE) for 1000 neutrons per cycle, 1000 cycles are shown in Table 2 for method 1 which includes first and second derivatives, and method 2 which uses only first derivatives.

Table 2: Predicted and actual Δk_{eff} vs Δu (RSE < 0.00005)

Δu	Predicted Δk_{eff} Method 1 Method 2	Re-run Δk_{eff}	Re-run k_{eff}
	Zone 1		
0.02	0.00366 0.00370	0.00693	1.00737 (0.00054)
0.05	0.00900 0.00925	0.01345	1.01389 (0.00052)
0.10	0.01749 0.01850	0.02504	1.02548 (0.00055)
	Zone 2		
0.02	0.00206 0.00208	0.00222	1.00266 (0.00053)
0.05	0.00506 0.00520	0.00553	1.00597 (0.00053)
0.10	0.00986 0.01040	0.0104	1.01084 (0.00053)
	Zone 3		
0.02	0.00072 0.00073	0.0007	1.00114 (0.00054)
0.05	0.00177 0.00182	0.00197	1.00241 (0.00241)
0.10	0.00345 0.00363	0.00348	1.00392 (0.00054)

The reference design in this section has enrichment u = 1.1%, for which k_{eff} = 1.00044 (0.00052). The perturbations are for fissile atomic densities N_5 = 7.6934 × 10^{19}, 7.8333 × 10^{19}, 8.0431 × 10^{19}, and 8.3928 × 10^{19} atoms cm^{-3} ($\frac{\delta N_5}{N_5}$ = 1.8%, 4.5%, 9.1%). The 'specific' change in k_{eff} for mass addition and mass removal, as well as the relative importance of each zone (relative to zone 1) are shown in Table 3.

Table 3: Δk_{eff} per unit mass U^{235} change

Zone	Mass addition $\frac{\Delta k_{eff}}{\Delta m_i}$ (10^{-3} kg^{-1})	Mass addition Importance	Mass removal $\frac{\Delta k_{eff}}{\Delta m_i}$ (10^{-3} kg^{-1})	Mass removal Importance
1	1.2163	1.0000	-1.2923	1.0000
2	0.5959	0.4899	-0.6692	0.5178
3	0.1874	0.1541	-0.2094	0.1620

Table 4: Optimal distribution from MC & GA

Zone	1	2	3	Total (kg)
x_i (kg)	14.755	1.306	-99.917	-83.856
Estimated optimal	187.655	174.206	72.983	434.844
Enrichment %	1.1939	1.1084	0.4643	-

From Table. 3, a random search was carried out using genetic algorithms (GA) and optimal values of Δm_i (for zone *i*) are obtained; results for mass vs. number of iterations (N) are shown in Table 4, Figure 5, and Figure 6. The convergence was obtained within 1000 iterations.

For mass changes in zone *i* specified as $0 \leq \Delta m_1, \Delta m_2 \leq 100$, and $-100 \leq \Delta m_3 \leq 100$, the MCM for the bare reactor is found as 434.844 kg with the maximum in the central zone and a progressive decrease toward the outer zone. Based on the zone importance alone, the mass additions x_i are 14.755 kg and 1.306 kg in zones 1 and 2 respectively, and mass removal 99.917 kg from zone 3 with a net savings of 83.856 kg (~16%) from the critical mass corresponding to uniform composition.

The convergence towards optimal MCM is shown in Figure 5 for the reactor and in Figure 6 for each of the zones.

For the distribution 1.1939%, 1.1%, and 0.5%, MCNP simulation gives $k_{eff} = 1.02165\ (0.00080)$ for a total fissile mass of 439.13 kg. System multiplication is estimated from re-runs with the following results: $k_{eff} = 1.00884\ (0.00088)$ at enrichment 1.15%, 1%, 0.5%, and at enrichments 1.12%, 1% and 0.5%. Thus, a material composition change is accurately predicted for a single region perturbation.

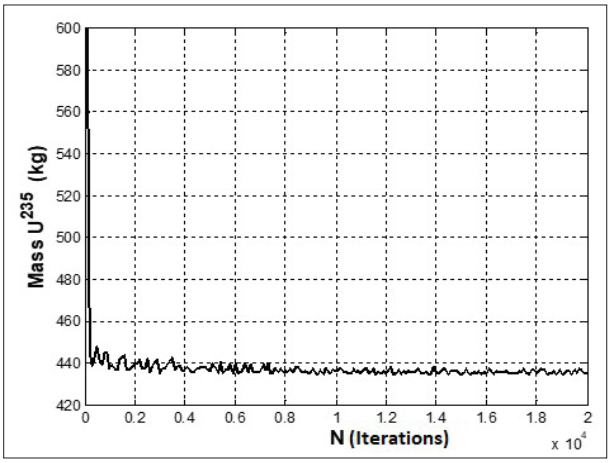

Figure 5: Minimum critical mass in a bare cylindrical reactor

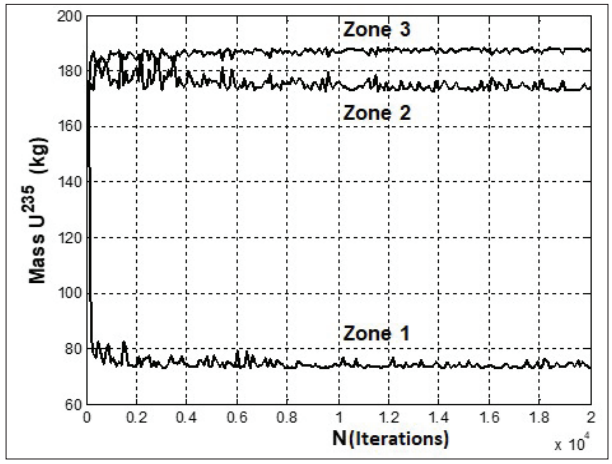

Figure 6: Optimal fissile distribution in a three-zone bare cylindrical reactor

Criticality experiment

We now consider experimental results for a U^{235}-H_2O multi-region criticality assembly (Clark, 1966). In the experiment, a cylindrical configuration with five regions separated by thin aluminium partitions of dimensions listed in Table 5, was surrounded by a 'thick' reflector laterally and no reflector at the top or bottom.

Table 5: Criticality experiment for U^{235}-H_2O

Region	I	II	III	IV	V
Inner radius (cm)	0	5.54	8.14	10.27	12.55
Outer radius (cm)	5.48	8.08	10.21	12.49	15.10

Table 6: Accuracy of perturbation estimates for concentration change

No.	Concentration (gU^{235}/L)	% change in k (Predicted)	σ_k	% change in k (Actual)	σ_k
1	43.769	2.7740	0.00006	2.699	0.00084
2	35.811	-3.1946	0.00007	-2.974	0.00078)

Table 7: Accuracy of perturbation estimates for mass addition

Zone	Concentration (gU^{25}/L)	% change in k (Predicted)	σ_k	% change in k (Actual)	σ_k
1	43.769	0.9927	0.00005	1.502	0.00082
2	43.769	0.8563	0.00003	0.9350	0.00077
3	43.769	0.9987	0.00003	0.6612	0.00079

Table 8: Predicted and actual changes Δk_{eff} for fissile mass addition by zone

Zone	Volume (L)	Mass (kg)	MU^5 (g)	M U^5 added (g)	Δk_{eff} Re-run and Predicted		
					Re-run	1st -order	1st & 2nd -order
1	4.02846	4.19644	160.29	16.027	0.00821	0.00458	0.00501
2	4.64075	4.83427	184.66	18.462	0.00686	0.00476	0.00459
3	5.09547	5.30795	202.75	20.272	0.00660	0.00481	0.00465
4	6.77802	7.06066	269.70	26.965	0.00628	0.00607	0.00587
5	9.45830	9.85271	376.35	37.628	0.00591	0.01006	0.00963
			1193.75	119.354	0.03386	0.03029	0.02817

The MC simulations for the criticality experiment with uniform concentration 39.79 gU^{235}/L estimated k_{eff} as 1.00637 (0.00080) while the effect of ±10% changes in concentration (g U^{235}/L) was predicted as shown in Table 6.

To estimate the reliability of the derivatives in a multi-region configuration, a simplified three-zone model of the criticality experiment is considered; the second-order derivatives were estimated for a 10% increase in concentration one zone at a time, for which the predictions were acceptable for the first two zones, as shown in Table 7. The third zone, however, gave an unreliable prediction for k_{eff} of ~1% for an actual change of ~0.7%.

Similar trends were observed in the full five-region MC simulation for the experiment, as shown in Table 8.

The reference concentration in each zone was 39.79 gU^{235}/L with criticality at 1193.75 g U^{235} distributed as shown above. With a 10% mass addition, one zone at a time, Δk_{eff} from re-runs was found to vary from 0.00821 in the first zone, decreasing to 0.00591 in the last zone. The predictions by 1st- and 2nd–order perturbation are at variance with the actuals and thus need to be corrected before they are used to estimate the optimal distribution. It is important to note that the overall prediction of a 10% mass increase is ~2.8% compared with an actual change of about ~3.4%. An estimate of the accuracy of prediction is the difference between the sum effect of individual changes in zones and the overall change in the system. The former gives $\Delta k_{eff} = \sum_{i=1}^{5} \Delta k_{eff_i} = +0.03426$ while an overall change gives 0.02818. There is a difference of ~18% which is the best accuracy that can be predicted by perturbation. The specific changes $\frac{\Delta k_{eff}}{\Delta m_i}$ are shown in Table 9 for mass additions and removals from individual zones.

Table 9: Δk_{eff} per unit mass U^{235} change

Zone	Mass addition		Mass removal	
	$\frac{\Delta k_{eff}}{\Delta m_i}$ (kg^{-1})	Importance	$\frac{\Delta k_{eff}}{\Delta m_i}$ (kg^{-1})	Importance
1	0.51851	1.0000	-0.37864	1.0000
2	0.37698	0.7271	-0.32380	0.85518
3	0.33051	0.6374	-0.28998	0.76584
4	0.23660	0.4563	-0.17758	0.46901
5	0.15706	0.3029	-0.13948	0.36837

Once the 'importance' of each zone is determined, the fissile material is added to the most important zone and others are subsequently filled. As this is done, the system multiplication k_{eff} will increase; thus, to bring the system back to criticality, the material can be removed from less important zones. The overall fissile mass in the system will be reduced if more material is removed from the less important zones than is added in the more important zones. Using the specific values $\frac{\Delta k_{eff}}{\Delta m_i}$ from Table 9, the optimum distribution results in a change of k_{eff} from k_{eff_u} = 0.9999 to k_{eff_o} = 1.0100 which is an error of ~1%. Thus, the re-runs give a reliable prediction of the optimal configuration. The optimal distribution is obtained using the derivatives from Table 9. For these, the uniform and optimal k_{eff} values of 0.9999 and 1.0101, with the net mass change being 127.99 g U^{235}, are estimated from $\sum_{i=1}^{5} \Delta k_{eff_i}$ for experimental optimal mass additions/removals from each zone. Thus, atomic densities for U^{235} should be in the ratios of zone importance, *i.e.*, cell importance normalized to zone 3 are 1.60, 1.14, 1, 0.72, and 0.47; thus the importance provides a good reference point for MC derivative sampling and

Table 10: Optimal distribution from MC & GA

Zone	1	2	3	4	5	Total (g)
x_i	100.004	60.012	5.011	-79.99	-230.043	-145.006
Est. Opt.	260.29	244.672	207.761	189.71	146.307	1048.74
Exp. Opt.	269.1	249.67	210.44	193.17	143.39	1065.77

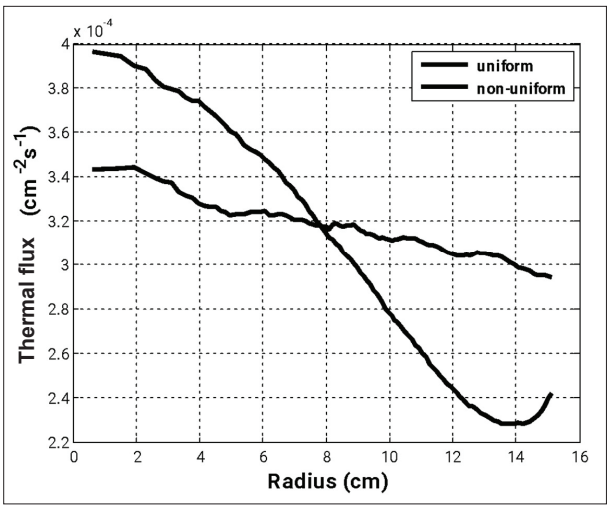

Figure 7: Thermal flux comparison uniform vs. optimal

perturbation estimates need to be corrected before being used for deciding which zone U^{235} should be added to or removed from.

Table 10 shows that a net removal of 145 g U^{235} is predicted by using correct derivatives to estimate an MCM of 1048.74 g U^{235} compared with the experimental MCM of 1065.77 g U^{235}, *i.e.*, a difference of 1.6%. The thermal flux for uniform and MCM (optimal) distributions are shown in Figure7 showing less peaking for the latter.

The correction factors are thus important for sampled derivatives to be used for estimating the zone importance and subsequently the optimal placement of fissile material.

CONCLUSIONS

The objective of this work was to estimate the reduction in critical mass in illustrative nuclear systems using results from a variational method and Monte Carlo (MC) simulation and particularly the derivatives obtained from a 'reference' MC computation. Optimization strategies were used for a bare cylindrical reactor with a restrictive condition giving 'critical' enrichment pairs. Reduced critical mass was obtained using derivative sampling for perturbation in a 'reference' design and Pontryagin's maximum principle in a variational formulation. Both these methods were applied and shown to estimate the minimum critical mass (MCM) for a bare cylindrical reactor and for a criticality experiment.

REFERENCES

Briesmeister J.F. (2003). *X-5 Monte Carlo Team: MCNP—A General Monte Carlo N-Particle Transport Code*. Los Alamos National Laboratory, Los Alamos, NM, USA.

Clark H.K. (1966). Effect of distribution of fissile material on critical mass. *Nuclear Science and Engineering* **24**(2): 133–141. DOI: https://doi.org/10.13182/NSE66-A18298

Dam H. (2013). Minimum critical mass in a heterogeneous thermal system. *Annals of Nuclear Energy* **53**: 221–227. DOI: https://doi.org/10.1016/j.anucene.2012.08.028

Dam H. (2015). On the anomaly in sizes of minimum critical mass cores. *Annals of Nuclear Energy* **86**: 23–28. DOI: https://doi.org/10.1016/j.anucene.2014.11.042

Goertzel G. (1956). Minimum critical mass and flat flux. *Journal of Nuclear Energy* **2**(3–4): 193–201. DOI: https://doi.org/10.1016/0891-3919(55)90034-6

Gosling F.G. (1999). *The Manhattan Project: making the atomic bomb*. Diane Publishing, Pennsylvania, USA.

Koreshi Z.U., Khan H., & Yaqub M. (2019). Variational methods and speed-up of Monte Carlo perturbation computations for optimal design in nuclear systems. *Nuclear Technology and Radiation Protection* **34**(3): 211–221. DOI: https://doi.org/10.2298/NTRP190214032K

Koreshi Z.U. & Lewins J.D. (1990). Two-group Monte Carlo perturbation theory and applications in fixed-source problems. *Progress in Nuclear Energy* **24**(1–3): 27–38. DOI: https://doi.org/10.1016/0149-1970(90)90020-6

Lamarsh J.R. & Baratta A.J. (2001). *Introduction to Nuclear Engineering*, 3rd edition, Prentice Hall Upper Saddle River, New Jersey, USA.

Lee C.K. (1973). Critical mass minimization of a cylindrical geometry reactor by two-group diffusion equation. *Nuclear Engineering and Technology* **5**(2): 115–131.

Lewins J. (2004). Minimum critical mass and flat flux in a 2-group model. *Annals of Nuclear Energy* **31**(5): 541–576. DOI: https://doi.org/10.1016/j.anucene.2003.09.001

Otsuka M. (2017). Fuel-importance function and minimum critical mass. *Nuclear Science and Engineering* **18**(4): 514–517. DOI: https://doi.org/10.13182/NSE64-A18770

Rief H. (1984). Generalized Monte Carlo perturbation algorithms for correlated sampling and a second-order Taylor series approach. *Annals of Nuclear Energy* **11**(9): 455–476. DOI: https://doi.org/10.1016/0306-4549(84)90064-1

Rowinski M.K., White T.J. & Zhao J. (2015). Small and medium sized reactors (SMR): A review of technology. *Renewable and Sustainable Energy Reviews* **44**: 643–656. DOI: https://doi.org/10.1016/j.rser.2015.01.006

Saracco P., Chentre N., Abrate N., Dulla S. & Ravetto P. (2019). Neutron multiplication and fissile material distribution in a nuclear reactor. *Annals of Nuclear Energy* **133**: 696–706. DOI: https://doi.org/10.1016/J.ANUCENE.2019.06.044

Segrè E. (1970). *Enrico Fermi, Physicist*. University of Chicago Press, Illinois, USA.

Szasz F.M. (1984). *The Day the Sun Rose Twice: The Story of The Trinity Site Nuclear Explosion*, *July 16, 1945*. University of New Mexico Press, New Mexico, USA.

Wilkins Jr., J.E. & Srivastava K.N. (1982). Minimum critical mass nuclear reactors. part II. *Nuclear Science and Engineering* ***82***(3): 316–324. DOI: https://doi.org/10.13182/NSE82-A19392

Williams M.M.R. (2003). Some Further Considerations on Goertzel's Minimum Critical Mass Problem. *Annals of Nuclear Energy* **30**(10): 1075–1088. DOI: https://doi.org/10.1016/S0306-4549(03)00014-8

Williams M.M.R. (2017). Conditions for a Minimum Critical Mass in a Nuclear Reactor and Considerations on Goertzel's Theorem in Transport Theory. *Nuclear Science and Engineering* **146**(2): 152–175.
DOI: https://doi.org/10.13182/NSE04-A2400

Annex 1

Notation	Description
$\hat{C}$	collision operator
D_i	diffusion coefficient, m
E	neutron energy, MeV
H	Hamiltonian
I_0	modified zero-order Bessel functions
$\tilde{J}$	objective function
J_0	zero-order Bessel function
K_0	modified zero-order Bessel function
$K(P' \rightarrow P)$	transfer kernel
N	atomic density
$\boldsymbol{P}(\vec{r}, \boldsymbol{\Omega}, E, t)$	phase space
R	radius, m
S_{ij}	coupling coefficient
$\hat{T}$	transport operator
V	volume
Y_0	zero-order Bessel function
f	distribution function
k_{eff}	effective multiplication factor
k_{∞}	infinite multiplication factor
m	fuel mass
p_i	coefficient in polynomial
p	resonance capture
r	radius, m
t	time
$u(r)$	control parameter
u	lethargy; $\left(\ln {}^{E_o}/_{E}\right)$
x	position
y	state variable
α	alpha particle
β	beta particle
γ	gamma ray
λ	Lagrange multiplier
μ	linear attenuation coefficient
τ_i	neutron age
ϕ_1	group-1 flux
ϕ_2	group-2 flux
χ(P)	collision denisty
φ_i	adjoint functions
ψ_i	Switching function
Σ_i	macroscopic cross-section (type i)
$\boldsymbol{\Omega}$	solid angle (steradians)
i	index for energy group or zone index
m	minimum
M	maximum